

# Highlights of Higgs Physics at LEP

**André Sopczak**  
Lancaster University

## **Abstract**

Final results from the combined data of the four LEP experiments ALEPH, DELPHI, L3 and OPAL on Standard Model (SM) Higgs boson searches are presented. New preliminary results of searches in extended models are reviewed.

Presented at the Fourth International Conference on Non-Accelerator New Physics,  
NANP-03, Dubna, Russia, 2003



# Highlights of Higgs Physics at LEP

André Sopczak  
Lancaster University  
E-mail: andre.sopczak@cern.ch

Final results from the combined data of the four LEP experiments ALEPH, DELPHI, L3 and OPAL on Standard Model (SM) Higgs boson searches are presented. New preliminary results of searches in extended models are reviewed.

The LEP experiments took data between August 1989 and November 2000 at centre-of-mass energies first around the Z resonance (LEP-1) and later up to 209 GeV (LEP-2). In 2000 most data was taken around 206 GeV. The LEP accelerator operated very successfully and a total luminosity of  $\mathcal{L} = 2461 \text{ pb}^{-1}$  was accumulated at LEP-2 energies. Data-taking ended on 3 November 2000, although some data excess was observed in searches for the SM Higgs boson with 115 GeV mass. In this report several different research lines are addressed: 1) the Standard Model Higgs boson: candidates, confidence levels, mass limit, coupling limits; 2) the Minimal Supersymmetric extension of the SM (MSSM): dedicated searches, three-neutral-Higgs-boson hypothesis, benchmark and general scan mass limits; 3) CP-violating models; 4) invisible Higgs boson decays; 5) flavour-independent hadronic Higgs boson decays; 6) neutral Higgs bosons in the general 2-doublet Higgs model; 7) Yukawa Higgs boson processes  $b\bar{b}h$  and  $b\bar{b}A$ ; 8) singly-charged Higgs bosons; 9) doubly-charged Higgs bosons; 10) fermiophobic Higgs boson decays  $h \rightarrow WW, ZZ, \gamma\gamma$ .

The results from Standard Model Higgs boson searches are final<sup>1</sup>, and the results of searches in extended models are mostly preliminary<sup>2</sup>. Limits are given at 95% CL.

## 1 Standard Model Higgs Boson

### 1.1 Combined Test Statistics and Candidates

Figure 1 shows that the observed SM excess is less than  $2\sigma$  for combined LEP data, and lists the final candidates. The excess is reduced compared to previous reports. A short summary of the development of the data excess was given previously<sup>3</sup>.

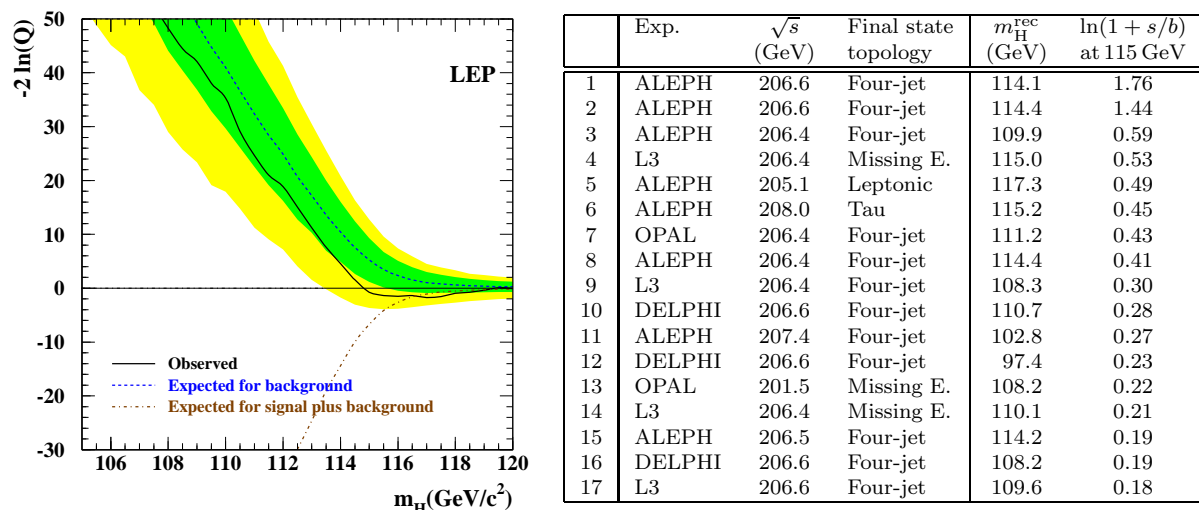


Figure 1: SM Higgs boson. Left: test statistics for the likelihood ratio  $Q = \mathcal{L}_{\text{signal+background}}/\mathcal{L}_{\text{background}}$ . The  $1\sigma$  and  $2\sigma$  error bands are indicated (shaded area). Right: final candidates. The signal  $s$  and background  $b$  estimates are used to construct an event weight  $\ln(1 + s/b)$ .

### 1.2 Test Statistics for Each Experiment

Figure 2 shows the test statistics for each experiment separately.

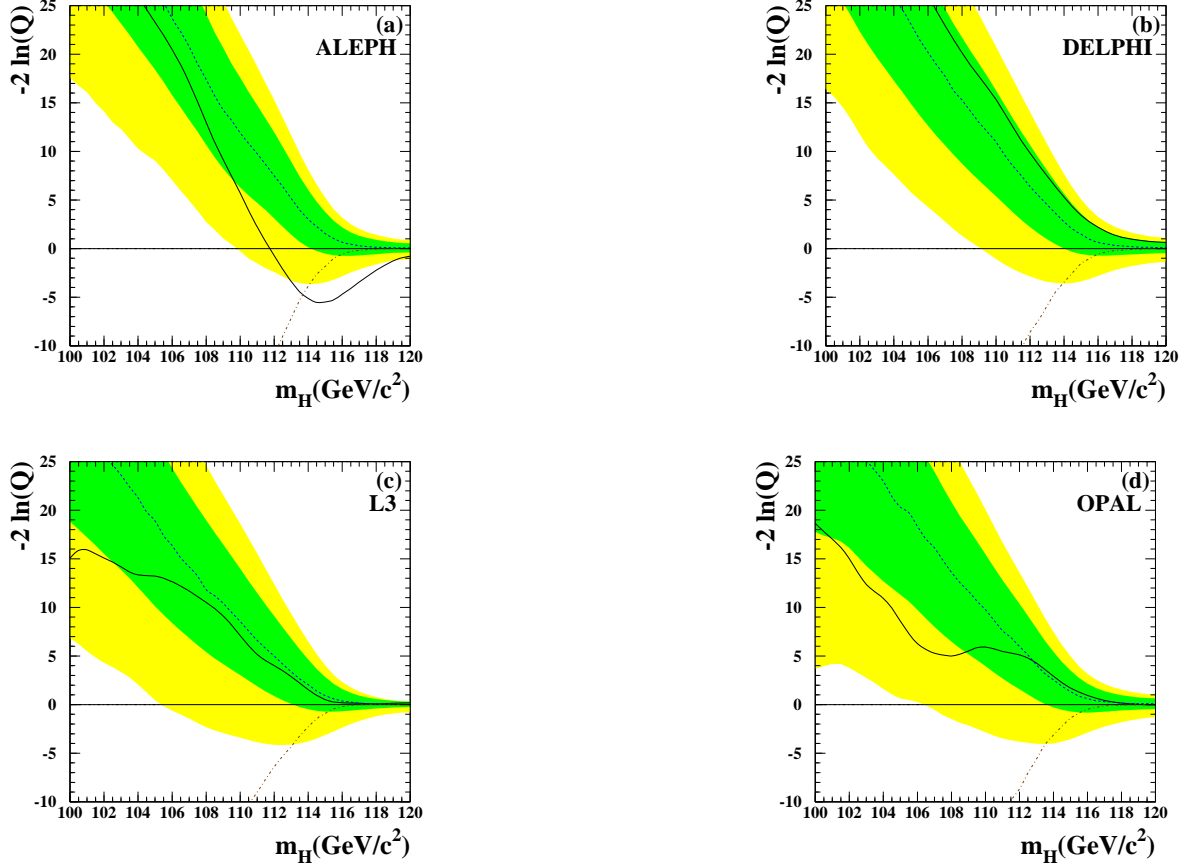


Figure 2: SM Higgs boson: test statistics for each experiment. As described in Fig. 1, solid line: data; dotted lines: expectation for background and for signal plus background.

### 1.3 Test Statistics for the Four-Jet and Other Channels

Figure 3 shows the test statistics for the four-jet channel and all other search channels combined.

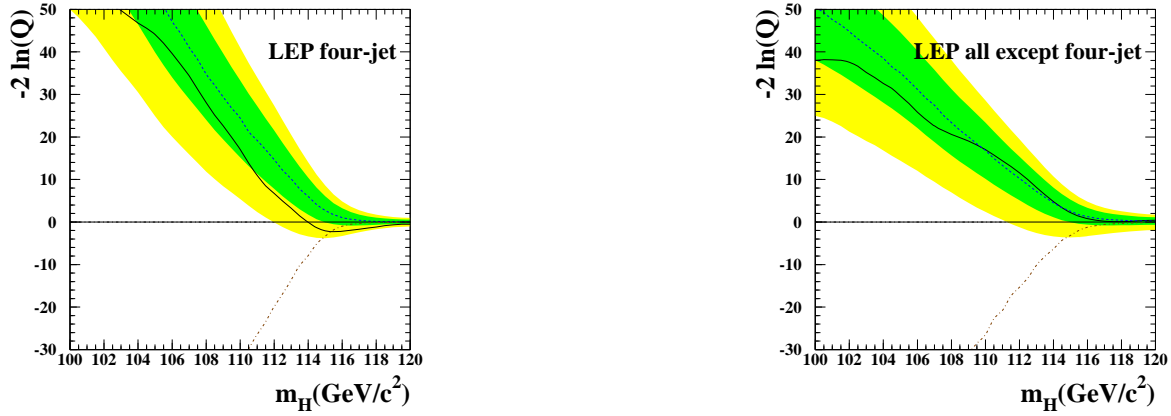


Figure 3: SM Higgs boson: test statistics for the four-jet channel and all other search channels combined. As described in Fig. 1, solid line: data; dotted lines: expectation for background and for signal plus background.

#### 1.4 Significance of Candidates for Each Experiment

Figure 4 shows the significance of the SM candidates as listed in Fig. 1 for each experiment separately as a function of the Higgs boson mass.

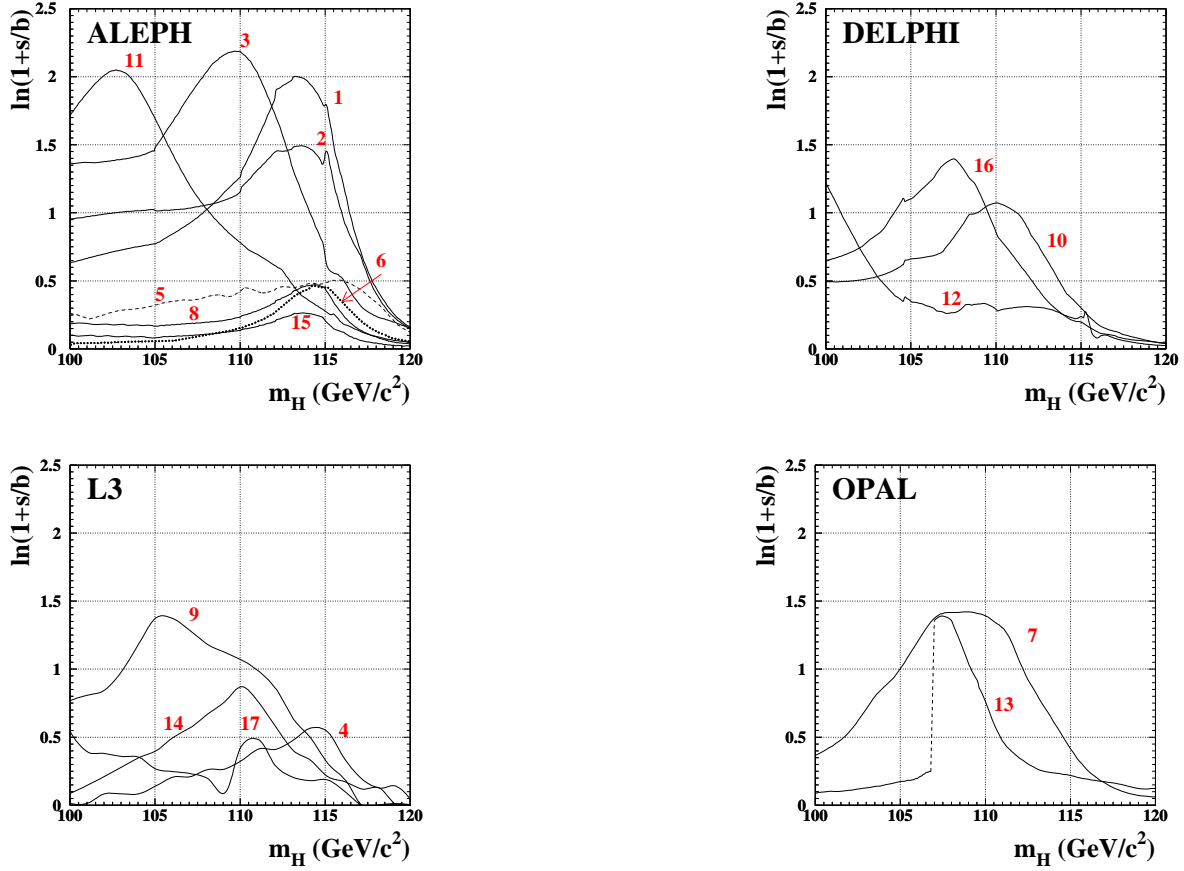


Figure 4: SM Higgs boson: significance of candidates as a function of the Higgs boson mass.

#### 1.5 Combined Significance of Candidates

Figure 5 shows the significance of the candidate events for a 110 GeV and 115 GeV Higgs boson hypothesis.

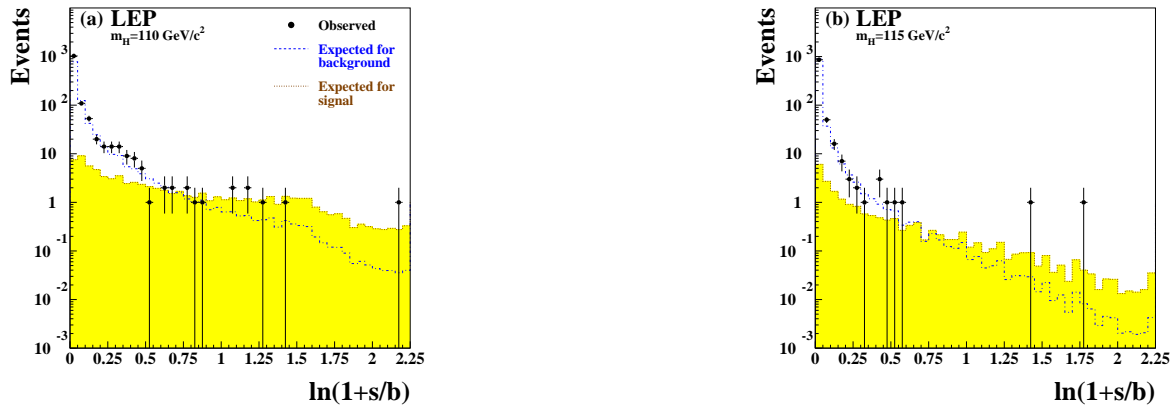


Figure 5: SM Higgs boson: significance of candidate events for a 100 GeV and 115 GeV Higgs boson hypothesis.

### 1.6 Reconstructed Candidate Masses

Figure 6 shows the reconstructed mass of the Higgs boson candidates with loose and tight selection cuts for a 115 GeV Higgs boson hypothesis.

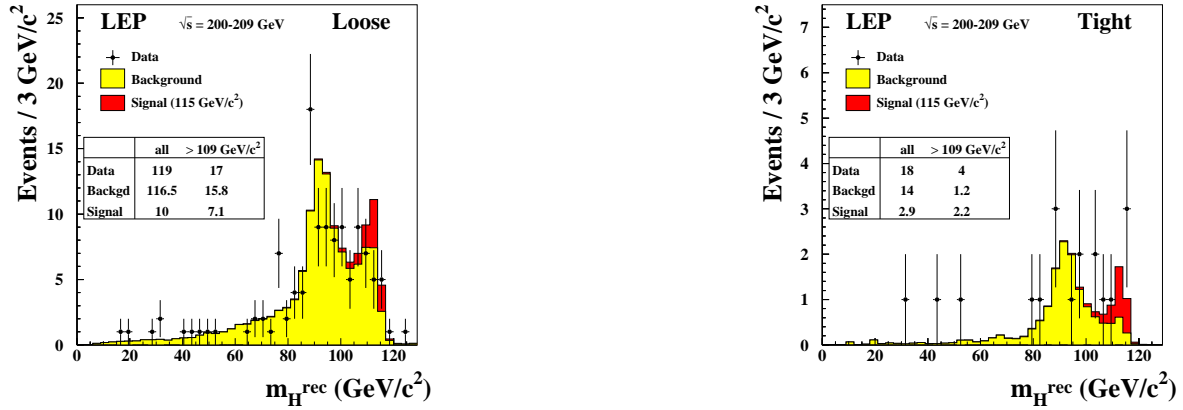


Figure 6: SM Higgs boson: reconstructed mass of Higgs boson candidates for loose and tight selection cuts.

### 1.7 Background Confidence Levels for Each Experiment

Figure 7 shows the confidence levels for background-only hypotheses for each experiment separately.

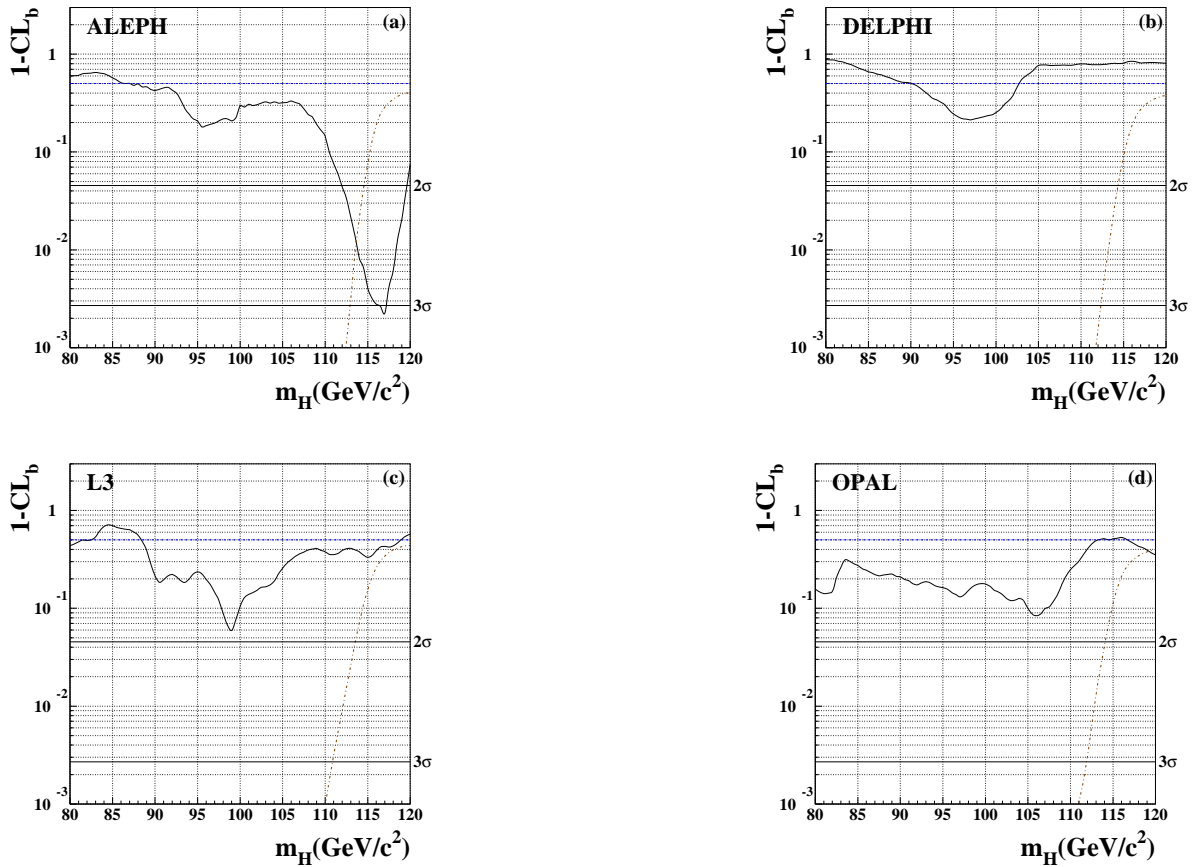


Figure 7: SM Higgs boson: confidence levels for background-only hypotheses for each experiment. The value  $1 - CL_b$  expresses the incompatibility of the observation with the background-only hypothesis.

### 1.8 Background Confidence Levels: About $2\sigma$ Deviations

Figure 8 shows a small data excess at 98 GeV in the four-jet channel and also in all other channels combined. In addition, a small excess at 115 GeV in the four-jet channel is observed.

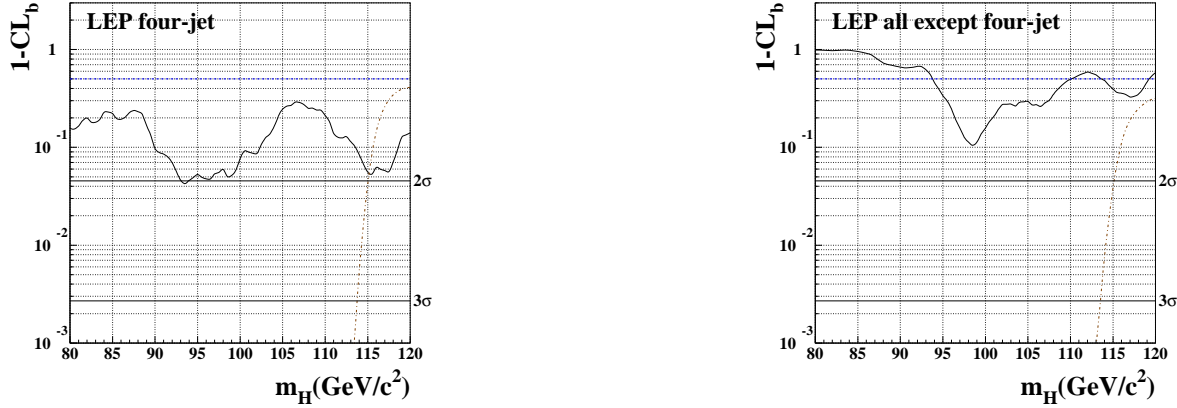


Figure 8: SM Higgs boson: a small data excess at 98 GeV in the four-jet and also in all other channels combined. In addition, a small excess at 115 GeV in the four-jet channel is observed.

### 1.9 Probability Densities for Signal and Background Hypotheses

Figure 9 shows the probability densities of the test statistics  $-2 \ln Q$  for background-only and signal plus background hypotheses for a 115 GeV Higgs boson, and the observed value of  $-2 \ln Q$ .

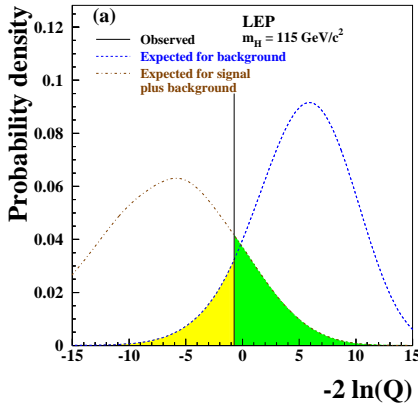


Figure 9: SM Higgs boson: probability densities of the test statistics  $-2 \ln Q$  for background-only and signal plus background hypotheses, and the observed value of  $-2 \ln Q$ .

### 1.10 Mass and Coupling Limits

Figure 10 shows the SM mass limit, and coupling limits assuming the Higgs boson decays with SM branching fractions and a SM production rate reduced by the factor  $\xi^2 = (g_{\text{HZZ}}/g_{\text{HZZ}}^{\text{SM}})^2$ .

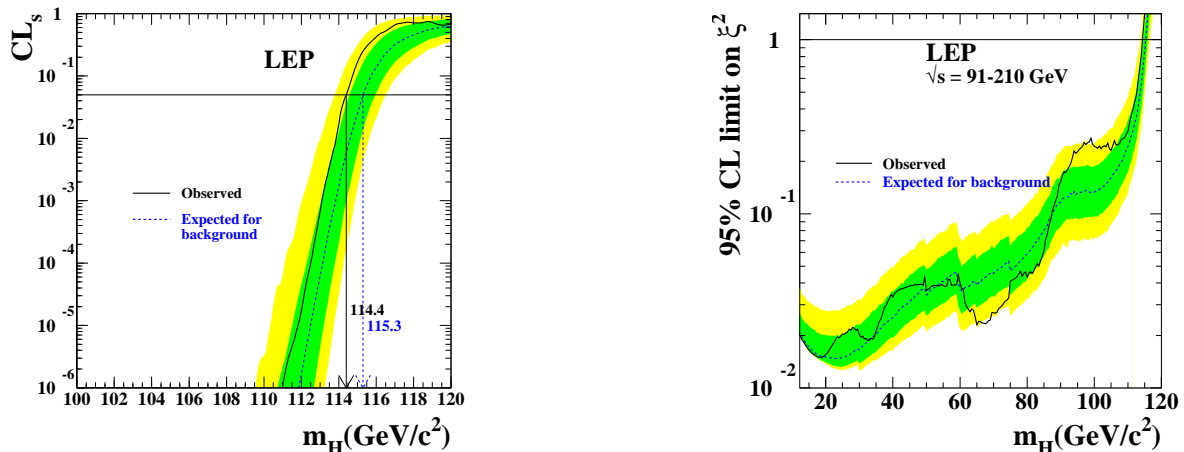


Figure 10: SM Higgs boson. Left: mass limit. Right: coupling limits assuming the Higgs boson decays with SM branching fractions and a SM production rate reduced by the factor  $\xi^2 = (g_{\text{HZZ}}/g_{\text{HZZ}}^{\text{SM}})^2$ .

### 1.11 Coupling Limits: $b$ -Quark and $\tau$ -Lepton Decay Modes

Figure 11 shows coupling limits for  $b$ -quark and  $\tau$ -lepton decay modes.

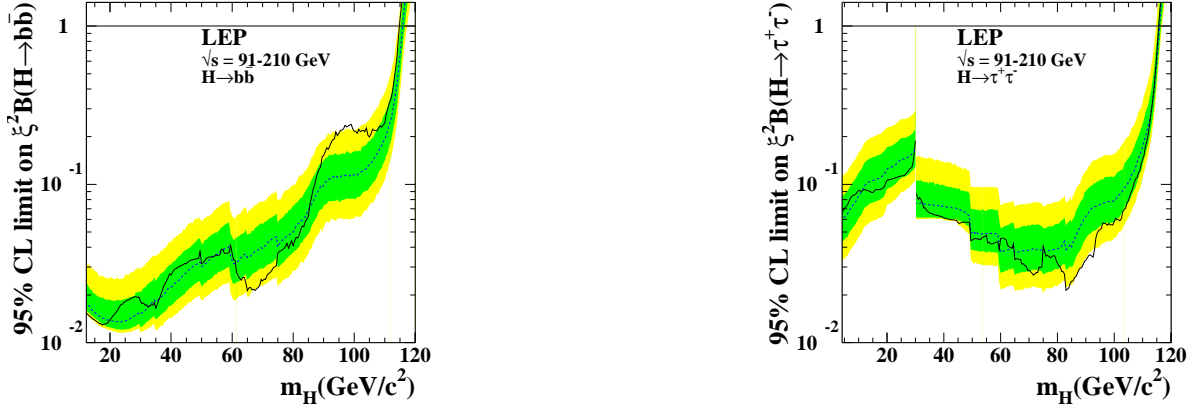


Figure 11: SM Higgs boson: coupling limits for  $b$ -quark and  $\tau$ -lepton decay modes.

## 2 Minimal Supersymmetric Extension of the SM (MSSM)

### 2.1 Benchmark Limits and Dedicated Low $m_A$ Searches

Figure 12 shows a previously small unexcluded mass region for light  $A$  masses in the no-mixing scalar top benchmark scenario. This region is mostly excluded by new dedicated searches for a light  $A$  boson (right plot).

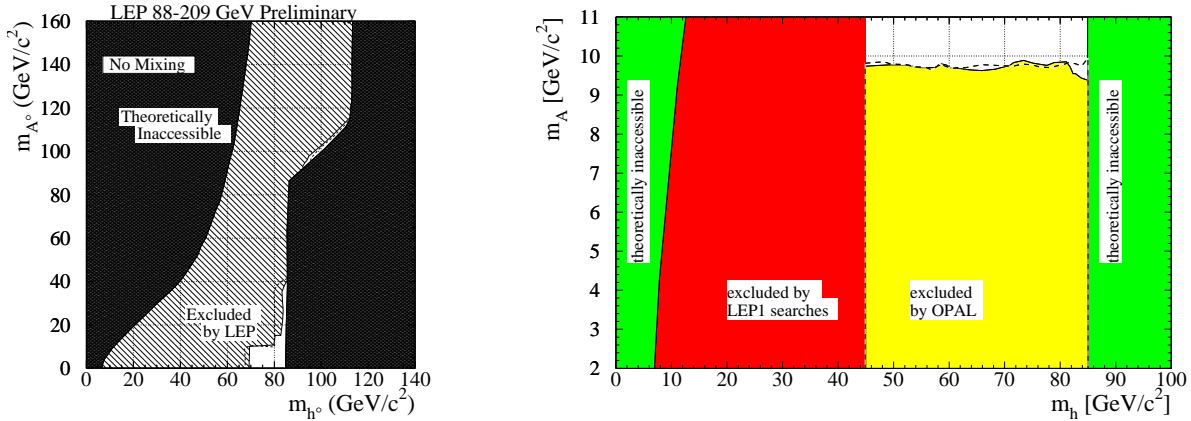


Figure 12: MSSM. Left: unexcluded mass region for a light  $A$  boson in the no-mixing scalar top benchmark scenario. Right: excluded mass region by dedicated searches for a light  $A$  boson.

### 2.2 Benchmark Limits and Dedicated $h \rightarrow AA$ Searches

Figure 13 shows mass limits for the maximum  $h$ -mass benchmark scenario, including results from dedicated searches for the reaction  $h \rightarrow AA$ .

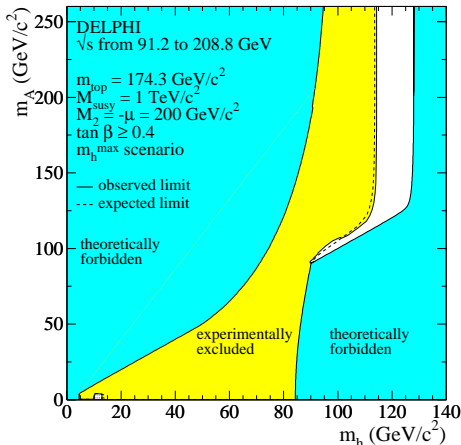


Figure 13: MSSM: excluded mass region for the maximum  $h$ -mass benchmark scenario, including results from dedicated searches for  $h \rightarrow AA$ .



### 2.3 Three-Neutral-Higgs-Boson Hypothesis

The hypothesis of three-neutral-Higgs-boson production, via  $hZ$ ,  $HZ$  and  $hA$  is compatible with the data excess seen in Fig. 14. For the reported MSSM parameters<sup>4</sup> reduced  $hZ$  production near 100 GeV and  $HZ$  production near 115 GeV is compatible with the data (left plot). For  $m_h \approx m_A$ ,  $hA$  production is also compatible with the data (right plot).

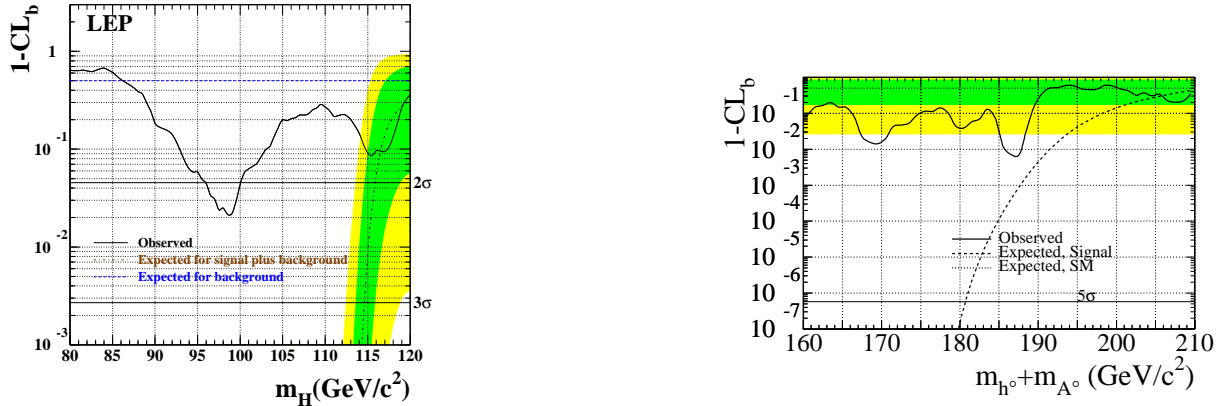


Figure 14: MSSM. Left: small data excess at 99 GeV and 116 GeV in  $hZ/HZ$  searches. Right: small data excess at  $m_h + m_A = 187$  GeV in  $hA$  searches.

### 2.4 MSSM Parameter Scan

Mass limits in the MSSM depend on invisibly-decaying Higgs boson searches, in particular for general MSSM parameter scans as shown in Fig. 15.

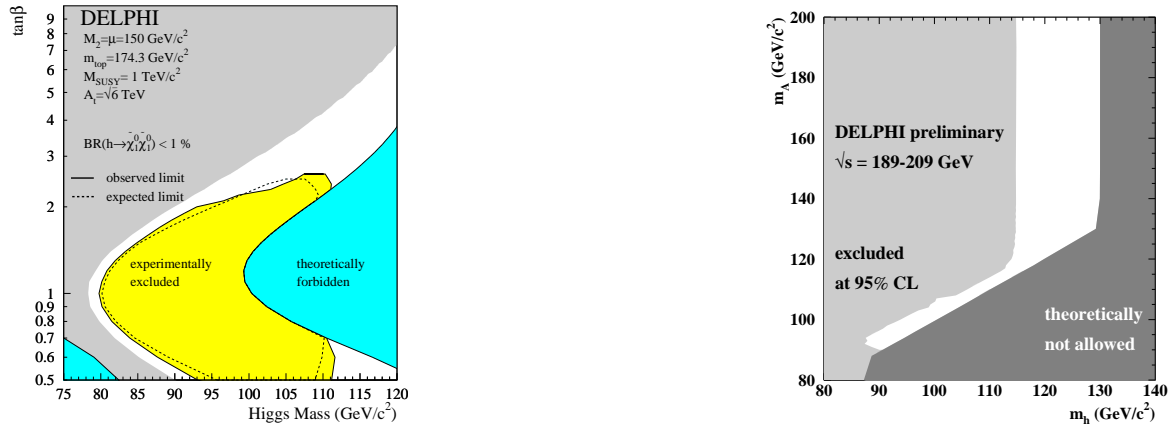


Figure 15: MSSM. Left: mass limits from searches for invisibly-decaying Higgs bosons. Right: mass limits from a general MSSM parameter scan.

## 3 CP-Violating Models

Instead of  $h$ ,  $H$  and  $A$ , the Higgs bosons are named  $H_1$ ,  $H_2$  and  $H_3$ . The reactions  $e^+e^- \rightarrow H_2 Z \rightarrow b\bar{b}\nu\bar{\nu}$  and  $e^+e^- \rightarrow H_2 Z \rightarrow H_1 H_1 Z \rightarrow b\bar{b}b\bar{b}\nu\bar{\nu}$  are searched for. No indication of these processes is observed in the data as shown in Fig. 16. Figure 17 from another study shows that a variation in CP-mixing reduces the MSSM mass limits significantly.

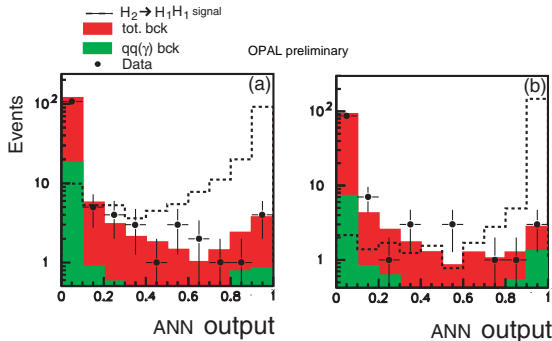


Figure 16: CP-violation models. Artificial Neural Network (ANN) output distributions for the reactions  $e^+e^- \rightarrow H_2 Z \rightarrow b\bar{b}\nu\bar{\nu}$  and  $e^+e^- \rightarrow H_2 Z \rightarrow H_1 H_1 Z \rightarrow b\bar{b}b\bar{b}\nu\bar{\nu}$  for different data sub-samples. No indication of a signal is observed.

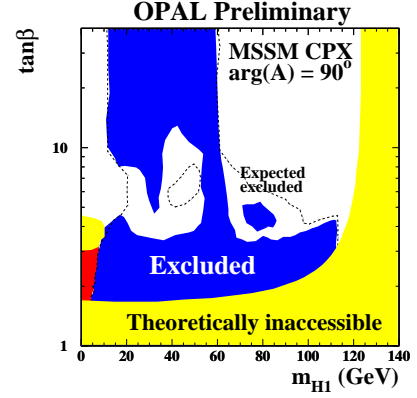
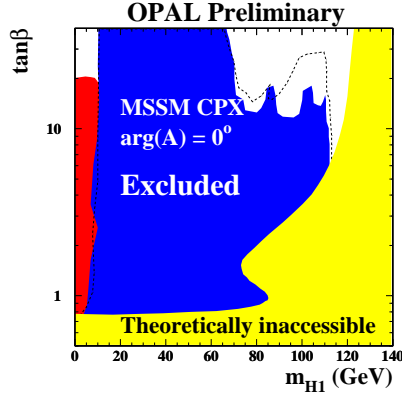


Figure 17: CP-violation models. Left: mass limits with no CP-mixing. Right: mass limits with full CP-mixing.

#### 4 Invisible Higgs Boson Decays

No indication of invisibly-decaying Higgs bosons is observed as shown in Fig. 18. Figure 19 shows mass limits for SM and invisible Higgs boson decays combined, and in Majoron models with an extra complex singlet,  $H/S \rightarrow JJ$ , where  $J$  escapes undetected.

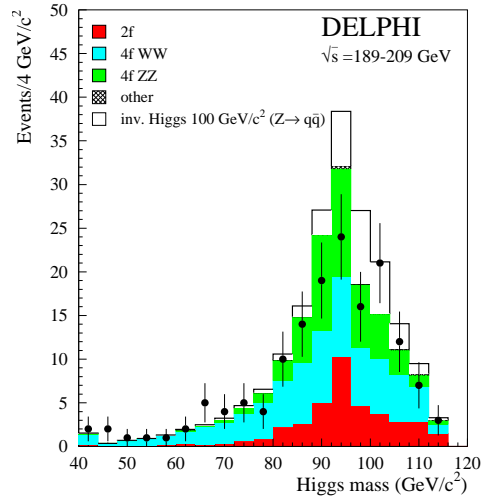
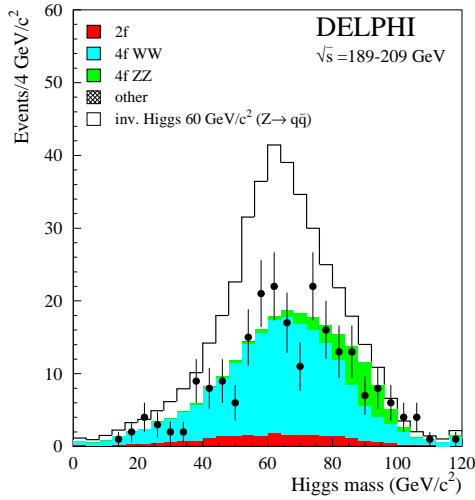


Figure 18: No indication of invisibly-decaying Higgs bosons is observed in searches optimized in low- and high-mass regions.

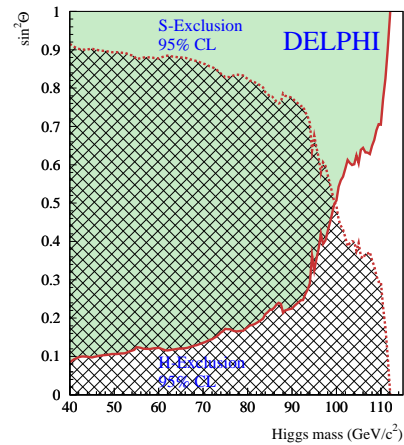
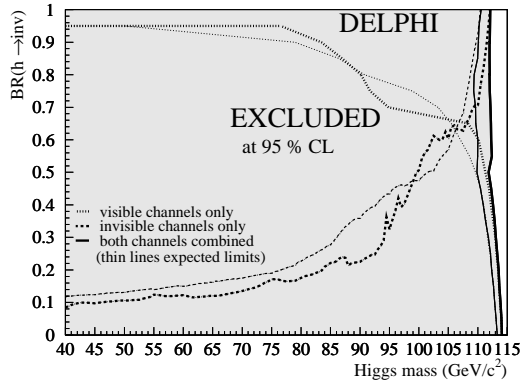


Figure 19: Left: mass limits for SM and invisible Higgs boson decays combined. Right: mass limits in Majoron models with an extra complex singlet,  $H/S \rightarrow JJ$ , where  $J$  escapes undetected.  $\sin^2 \theta$  is the  $H/S$  mixing angle.

## 5 Flavour-Independent Hadronic Higgs Boson Decays

Figure 20 shows no indication of a signal for the process  $hZ \rightarrow q\bar{q}\ell^+\ell^-$  above the background  $ZZ \rightarrow q\bar{q}\ell^+\ell^-$ . In addition, the expected signal efficiencies are shown. Flavour-independent limits from searches for hadronic  $hZ$  and  $hA$  decays are shown in Fig. 21.

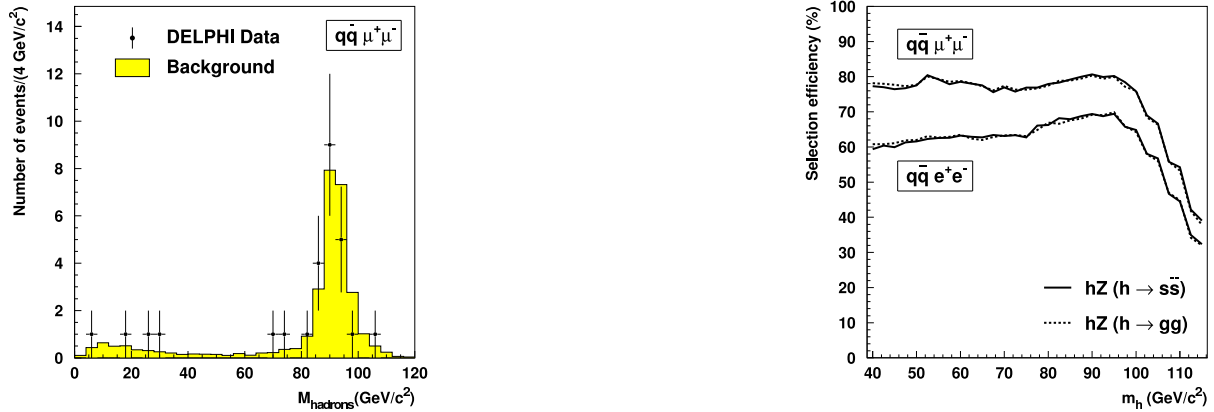


Figure 20: Left: no indication of a signal for the process  $hZ \rightarrow q\bar{q}\ell^+\ell^-$  above the background  $ZZ \rightarrow q\bar{q}\ell^+\ell^-$ . Right: expected signal efficiencies.

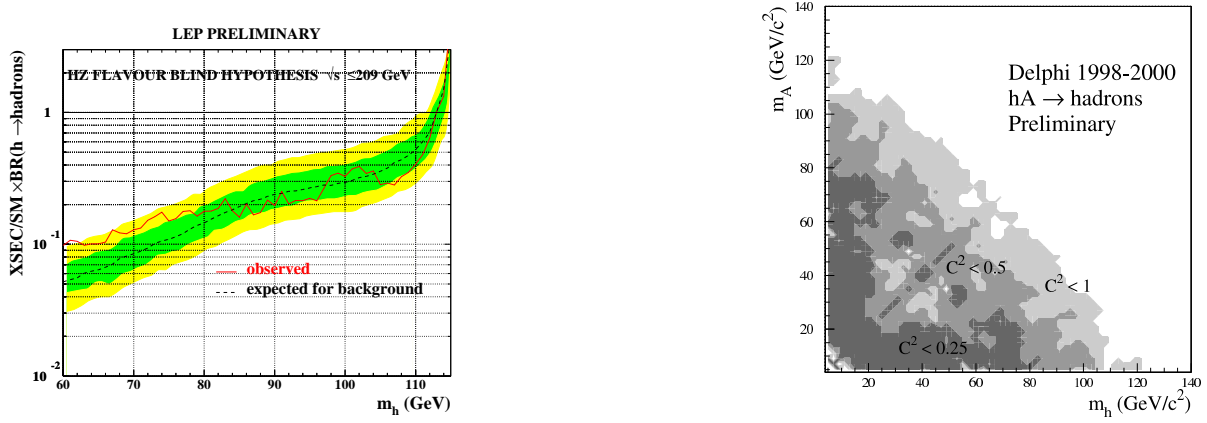


Figure 21: Flavour-independent limits from searches for hadronic  $hZ$  and  $hA$  decays. No  $b$ -tagging requirement is applied.  $C^2$  is the reduction factor on the maximum production cross section.

## 6 Neutral Higgs Bosons in the General 2-Doublet Higgs Model (2DHM)

Figure 22 shows mass limits from dedicated searches for  $hA$  production and from a parameter scan. The scan combines searches with  $b$ -tagging and flavour-independent searches.

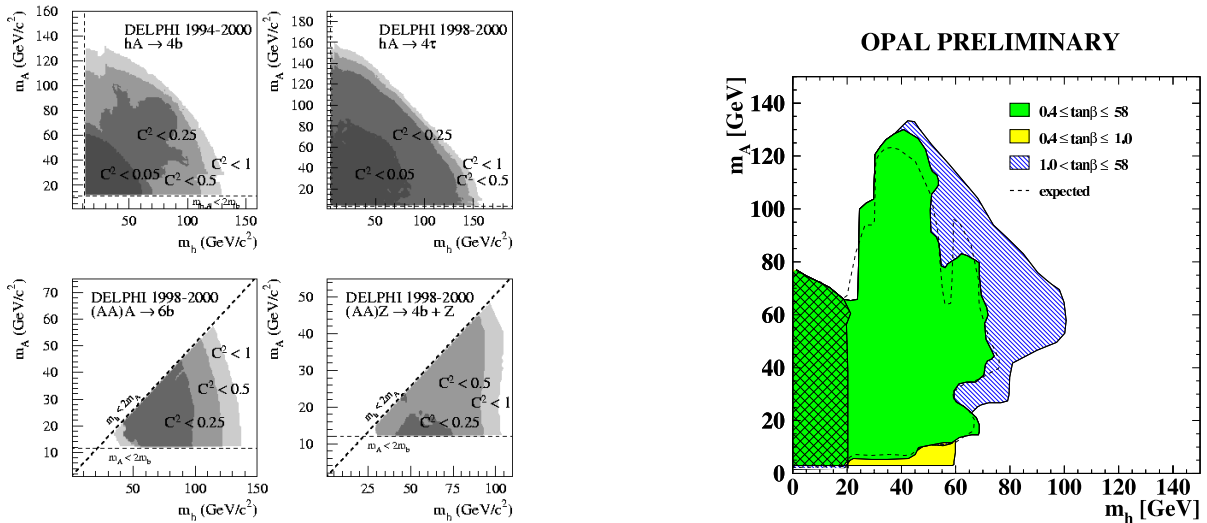


Figure 22: 2DHM. Left: mass limits from dedicated searches for  $hA$  production.  $C^2$  is the reduction factor on the maximum production cross section. Right: mass limits from a general 2DHM parameter scan.

## 7 Yukawa Higgs Boson Processes $b\bar{b}h$ and $b\bar{b}A$

Figure 23 shows mass limits from searches for the Yukawa processes  $e^+e^- \rightarrow b\bar{b} \rightarrow b\bar{b}h$ ,  $b\bar{b}A$ .

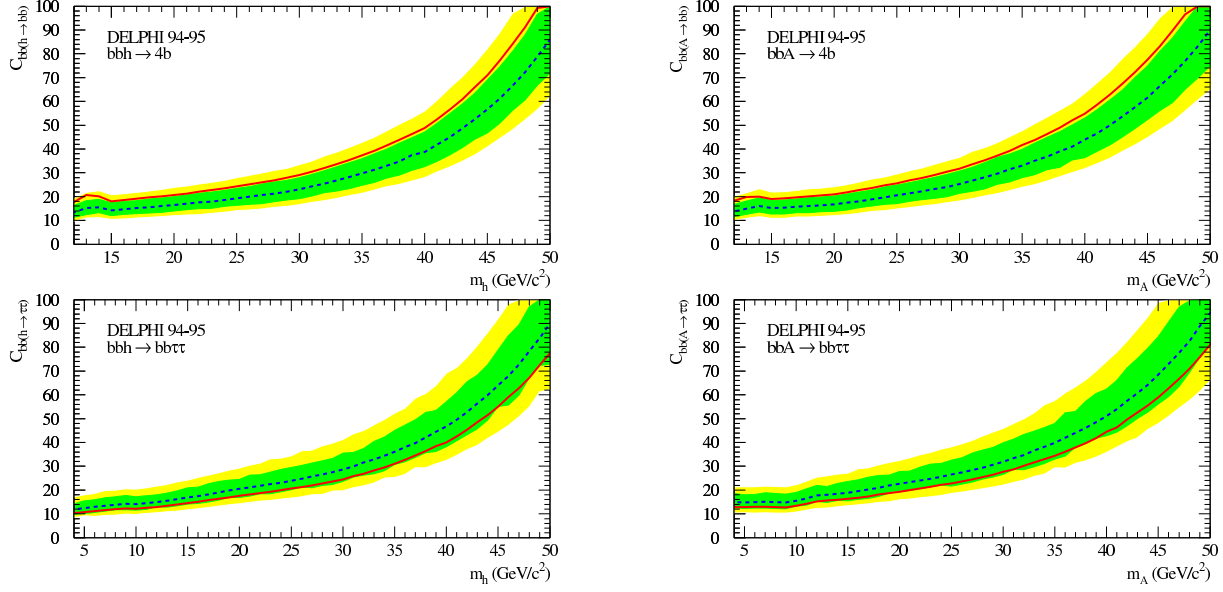


Figure 23: Observed (solid line) and expected (dotted line) mass limits from searches for the Yukawa processes  $e^+e^- \rightarrow b\bar{b} \rightarrow b\bar{b}h$ ,  $b\bar{b}A$ . The  $C$  factors include vertex enhancement factors and decay branching fractions.

## 8 Singly-Charged Higgs Bosons

Figure 24 shows mass limits from searches for  $e^+e^- \rightarrow H^+H^- \rightarrow c\bar{s}cs$ ,  $c\bar{s}\tau\nu$ ,  $\tau^+\nu\tau^-\bar{\nu}$ . The decay  $H^\pm \rightarrow W^\pm A$  could be dominant and limits from searches for the process are shown in Fig. 25.

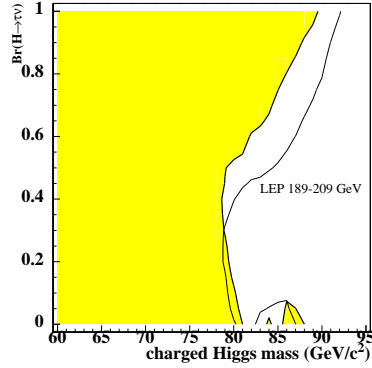


Figure 24: Excluded mass region (shaded area) from searches for  $e^+e^- \rightarrow H^+H^- \rightarrow c\bar{s}cs$ ,  $c\bar{s}\tau\nu$  and  $\tau^+\nu\tau^-\bar{\nu}$ . The thin line shows the expected limit.

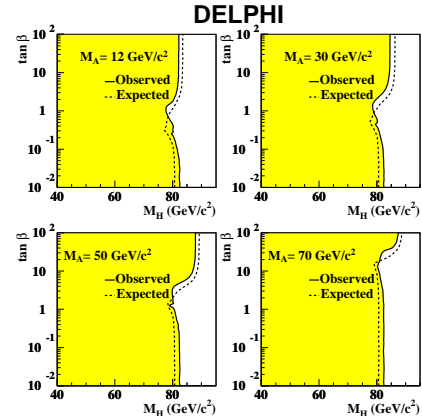
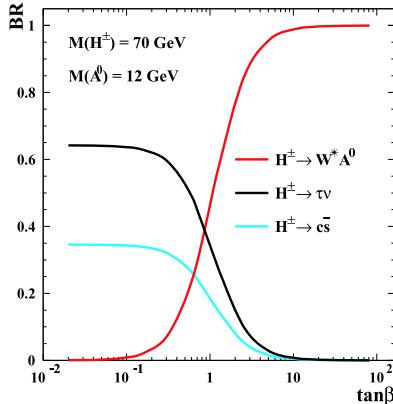


Figure 25: Left:  $H^\pm \rightarrow W^\pm A$  decays could be dominant for light  $A$  boson masses. Right: excluded mass region (shaded area) from searches for this process.

## 9 Doubly-Charged Higgs Bosons

The process  $e^+e^- \rightarrow H^{++}H^{--} \rightarrow \tau^+\tau^+\tau^-\tau^-$  can lead to decays at the primary interaction point ( $h_{\tau\tau} \geq 10^{-7}$ )<sup>5,6</sup>, a secondary vertex, or stable massive particle signatures. Figure 26 shows no indication of a signal in the data. Limits on the production cross section are given in Fig. 27.

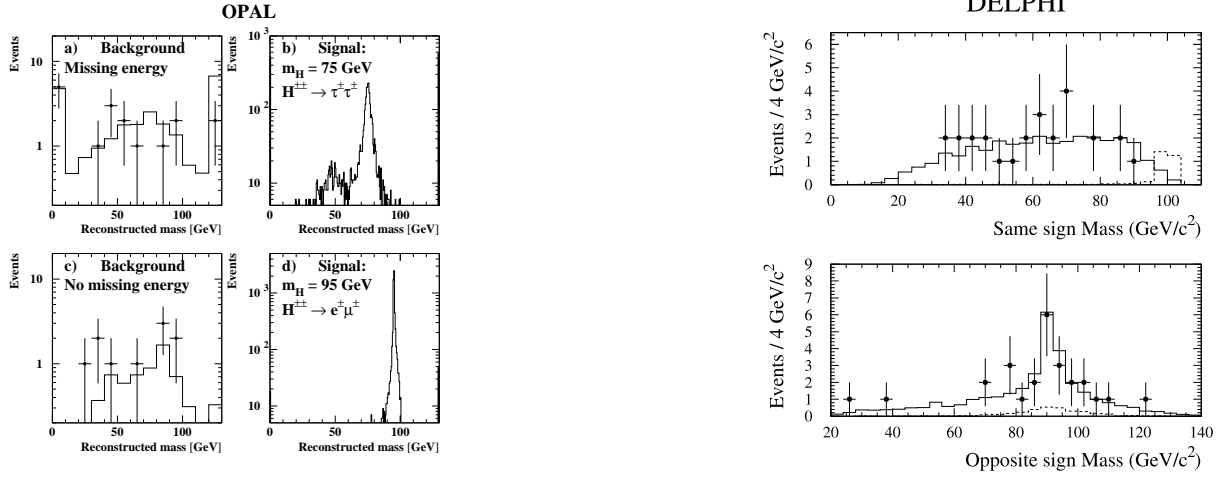


Figure 26: No indication of  $e^+e^- \rightarrow H^{++}H^{--} \rightarrow \tau^+\tau^+\tau^-\tau^-$  is observed in the data.

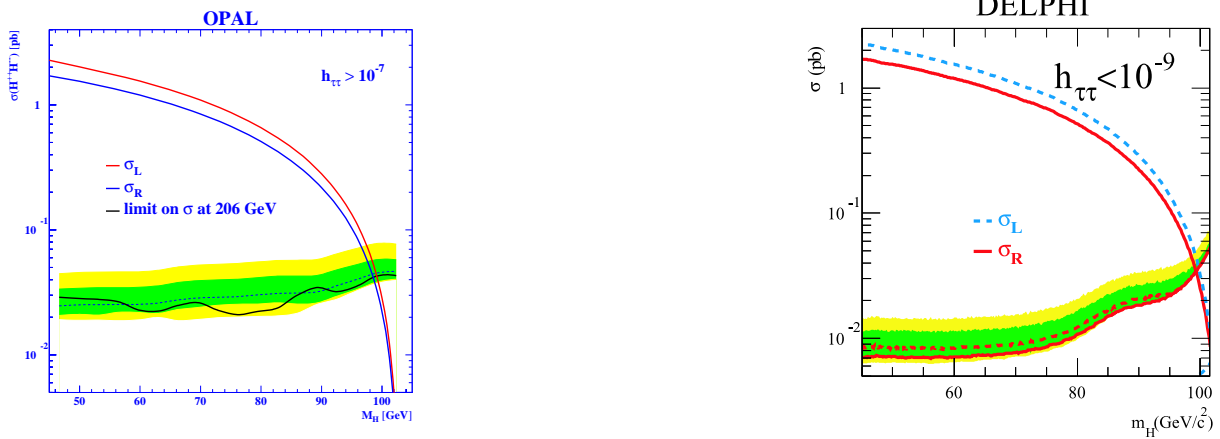


Figure 27: Limits on the  $e^+e^- \rightarrow H^{++}H^{--}$  production cross section are set as a function of the doubly-charged Higgs boson mass.

## 10 Fermiophobic Higgs Boson Decays: $h \rightarrow WW, ZZ, \gamma\gamma$

If Higgs boson decays into fermions are suppressed,  $h \rightarrow WW, ZZ, \gamma\gamma$  decays could be dominant. Mass limits from dedicated searches are shown in Fig. 28.

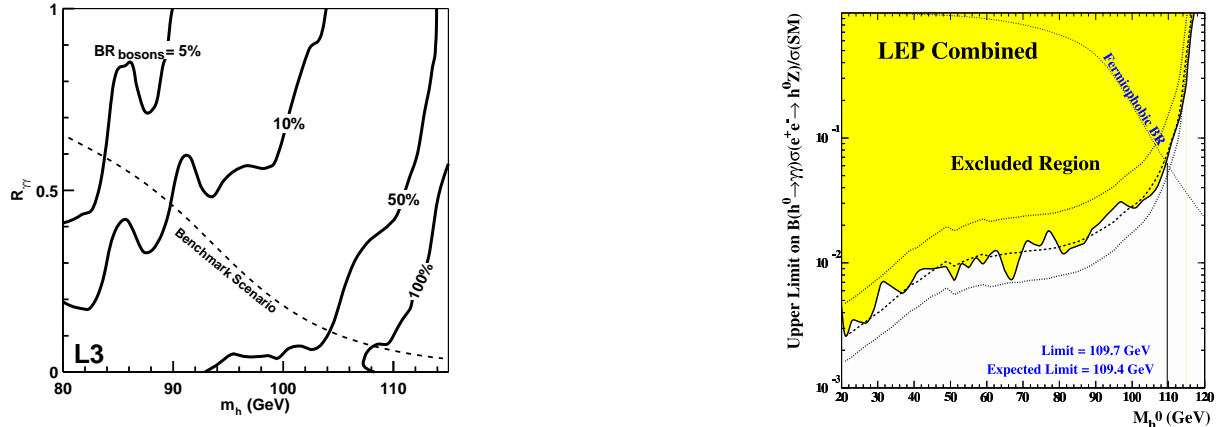


Figure 28: Left: mass limits as defined in Ref. <sup>7</sup> from  $h \rightarrow WW, ZZ, \gamma\gamma$  searches. Right: mass limits from  $h \rightarrow \gamma\gamma$  combined results.

## 11 Conclusions

Immense progress over a period of 14 years has been made at LEP in searches for Higgs bosons and much knowledge has been gained in preparation for new searches. No signal has been observed and various stringent limits are set as summarized in Table 1.

Table 1: Summary of Higgs boson mass limits at 95% CL.

Search	Experiment	Limit
Standard Model	LEP	$m_H^{\text{SM}} > 114.4 \text{ GeV}$
Reduced rate and SM decay		$\xi^2 > 0.05 : m_H > 85 \text{ GeV}$
		$\xi^2 > 0.3 : m_H > 110 \text{ GeV}$
Reduced rate and $b\bar{b}$ decay		$\xi^2 > 0.04 : m_H > 80 \text{ GeV}$
		$\xi^2 > 0.25 : m_H > 110 \text{ GeV}$
Reduced rate and $\tau^+\tau^-$ decay		$\xi^2 > 0.2 : m_H > 113 \text{ GeV}$
MSSM (no scalar top mixing)	LEP	almost entirely excluded
General MSSM scan	DELPHI	$m_h > 87 \text{ GeV}, m_A > 90 \text{ GeV}$
CP-violating	OPAL	strongly reduced limits
Visible/invisible Higgs decays	DELPHI	$m_H > 111.8 \text{ GeV}$
Majoron model (max. mixing)		$m_{H,S} > 112.1 \text{ GeV}$
Flavour-ind. hadronic decay (for $\sigma_{\text{max}}$ )	LEP	$hZ \rightarrow q\bar{q} : m_H > 112.9 \text{ GeV}$
	DELPHI	$hA \rightarrow q\bar{q}q\bar{q} : m_h + m_A > 110 \text{ GeV}$
2DHM (for $\sigma_{\text{max}}$ )	DELPHI	$bbbb : m_h + m_A > 150 \text{ GeV}$
		$\tau^+\tau^-\tau^+\tau^- : m_h + m_A > 160 \text{ GeV}$
		$(AA)A \rightarrow 6b : m_h + m_A > 150 \text{ GeV}$
		$(AA)Z \rightarrow 4b : m_h > 90 \text{ GeV}$
General 2DHM scan	OPAL	$\tan \beta > 1 : m_h \approx m_A > 85 \text{ GeV}$
Yukawa process	DELPHI	$C > 40 : m_{h,A} > 40 \text{ GeV}$
Singly-charged Higgs bosons	LEP	$m_{H^\pm} > 78.6 \text{ GeV}$
$W^\pm A$ decay mode	DELPHI	$m_{H^\pm} > 76.7 \text{ GeV}$
Doubly-charged Higgs bosons	DELPHI/OPAL	$m_{H^{++}} > 99 \text{ GeV}$
Fermiophobic $H \rightarrow WW, ZZ, \gamma\gamma$	L3	$m_H > 108.3 \text{ GeV}$
$H \rightarrow \gamma\gamma$	LEP	$m_H > 109.7 \text{ GeV}$

## Acknowledgments

I would like to thank the organizers of the NANP03 conference for their kind hospitality, and Tom Junk and Bill Murray for comments on the manuscript.

## References

1. ALEPH, DELPHI, L3 and OPAL Collaborations and the LEP working group for Higgs boson searches, Phys. Lett. **B 565** (2003) 61.
2. ALEPH, DELPHI, L3 and OPAL Collaborations, contributed papers to the International Europhysics Conference on High Energy Physics EPS, 17-23 July 2003, Aachen, Germany; and XXI International Symposium on Lepton and Photon Interactions at High Energies, 11-16 August 2003, Fermi National Accelerator Laboratory, Batavia, Illinois, USA.
3. A. Sopczak, Proc. NANP01, Phys. Atom. Nucl. **65** (2002) 2116.
4. A. Sopczak, Proc. DPF-2000, hep-ph/0011285.
5. DELPHI Collaboration, J. Abdallah et al., Phys. Lett. **B 552** (2003) 127.
6. OPAL Collaboration, G. Abbiendi et al., Phys. Lett. **B 577** (2003) 93.
7. L3 Collaboration, P. Achard et al., Phys. Lett. **B 568** (2003) 191.